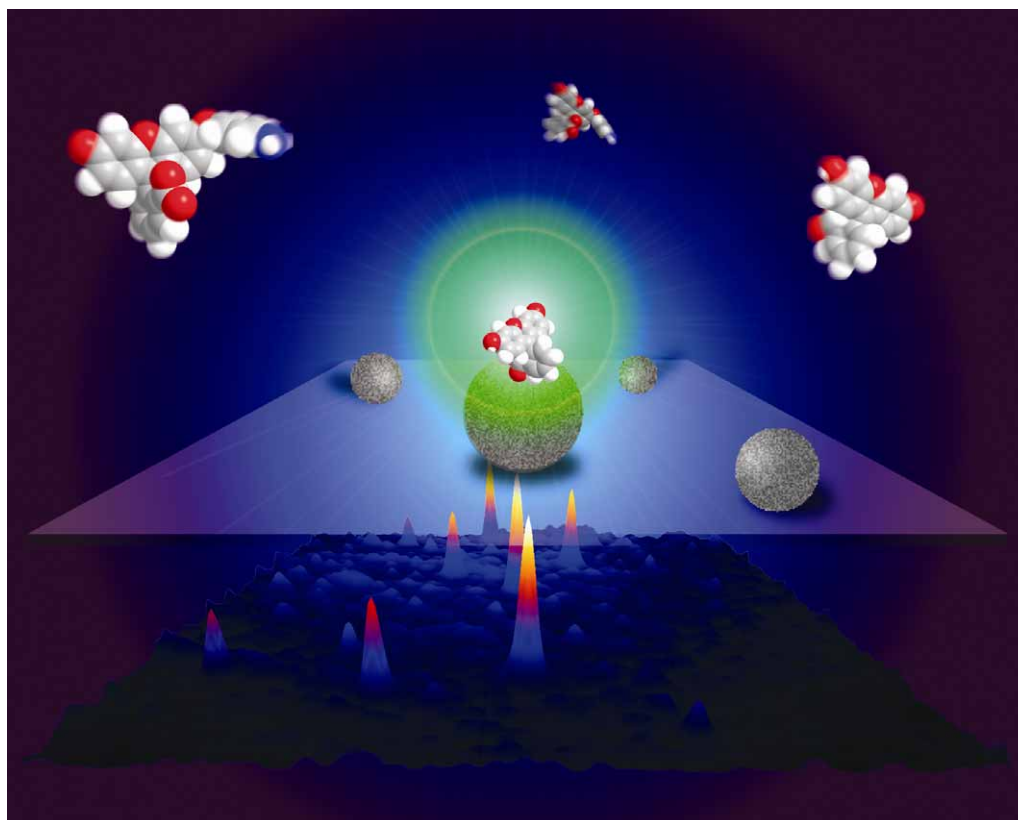# Chem Soc Rev

This article was published as part of the

In-situ characterization of heterogeneous catalysts themed issue

Guest editor Bert M. Weckhuysen

Please take a look at the issue 12 2010 table of contents to access other reviews in this themed issue

The role of synchrotron radiation in examining the self-assembly of crystalline nanoporous framework materials: from zeolites and aluminophosphates to metal organic hybrids†

Matthew G. O'Brien, Andrew M. Beale and Bert M. Weckhuysen*

This *tutorial review* describes the role of synchrotron-based techniques in the study of the formation of Crystalline Nanoporous Framework Materials (CNFMs), such as zeolites, aluminophosphates (AlPOs) and metal organic frameworks (MOFs). Initially, a general formation process for CNFMs is described and the 'tool kit' (including synchrotron and non-synchrotron-based techniques) used to examine this complex process is presented. The need for realistic *in situ* conditions and the balance between this, data quality and time resolution, are also discussed with reference to commonly utilized *in situ* synchrotron-based experimental cells. The experimental studies into the formation of several CNFM systems are then examined and the role of the synchrotron-based experiments, in context with those obtained from other techniques, is discussed. From this the importance of the synchrotron-based technique is demonstrated, however it is also shown that, to obtain a more complete understanding of the formation process, complementary independent measurements are still often required. During these discussions some of the most common experimental techniques and analytical methods are also discussed in detail and critically assessed.

1. Introduction

Crystalline Nanoporous Framework Materials (CNFMs) have formed an integral part of both academic and industrial materials science over the past half a century. It is the nanometer length scale of the pores within these materials, together with the ability to modify and functionalize their structural frameworks which continue to hold both

Inorganic Chemistry and Catalysis Group, Debye Institute for NanoMaterials Science, Utrecht University, Sorbonnelaan 16, 3584 CA Utrecht, The Netherlands
† Part of the themed issue covering recent advances in the *in-situ* characterization of heterogeneous catalysts.

fascination for academics and promise for industrialists. When these properties are properly married, CNFMs such as zeolites and aluminophosphates (AlPOs) have found utilization in areas as diverse as water softening, environmental cleanup, catalytic cracking and the production of 'value added' products such as olefins and gasoline.[1] More recently, the development of metal organic frameworks (MOFs) has opened up new fields of research and offer interesting opportunities in areas such as bio-catalytic mimicking, gas-storage and photoluminescence.[2,3]

There is no doubt that the discovery of new CNFMs is at the forefront of materials research and, from the inception of the field, *experimental* research has tended to rely on either high throughput 'brute force' experiments or on a

Matthew G. O'Brien (31) earned his masters degree in chemistry at the University College London (UCL, United Kingdom) and obtained his PhD entitled 'Investigations into the Formation of Nanoporous Materials' from UCL and the Royal Institution of Great Britain under the supervision of Prof. C. R. A. Catlow. He is currently working as a post-doctoral research fellow at Utrecht University (The Netherlands) in the group of Prof. B. M. Weckhuysen, where he investigates a variety of catalytic processes through the use of synchrotron-based techniques.

Matthew G. O'Brien

Andrew M. Beale (35) was born in Beckenham (UK) and went on to study Chemistry at Sussex University (United Kingdom) followed by a PhD in 2003 from University College London (United Kingdom). Since 2004 he has been based in the department of Inorganic Chemistry and Catalysis, Utrecht University (The Netherlands), first as a post-doctoral fellow and subsequently (2009) as Assistant Professor in the group of Professor Bert M. Weckhuysen. His research interests lie in the studying of catalytic processes using in situ/operando spectroscopic and scattering methods.

Andrew M. Beale

This journal is © The Royal Society of Chemistry 2010

Chem. Soc. Rev., 2010, **39**, 4767–4782 | 4767

'trial and error' variation of known synthesis parameters (*Computational* research has of course also played a hugely significant role in our understanding of these process and in some cases the results of this work have identified the conditions required to synthesize new zeolites.[4] For more details on this large body of work see Auerbach *et al.*[5]). Trial and error represents partial rationalization in design and depends considerably on previous literature (*i.e.* comparison between different synthesis components and conditions and the final product) and the complexity of the particular system under examination. For example, the synthesis of inorganic CNFMs has been widely studied but is a complex process, limiting the possibilities for rationalization. This has resulted in a large number of zeolite structures (*i.e.* 179)[6] but with only a few (*i.e.* 18) finding commercial use.[7] On the other hand MOFs remain relatively un-explored, however the apparently simple metal 'node' and organic 'linker' synthesis concepts[8] have allowed a more rational design and control over some parameters such as the pore size (*i.e.* the isorectulinear edge expansion through insertion of longer chained linkers).[9]

Ultimately one can envisage an ideal world in which the design of a new CNFM is fully rationalized and constructed to specification through knowledge of the product required (*e.g.* shape and size of the pores), the building blocks available and the chemical and physical processes required to bring the structure together. The nanomaterials scientist would then be able to efficiently target the development of materials with a pore structure and orientation of use for applications such as catalysis, gas storage and separation. Given the complexity of the formation process however, the completion of such a 'synthesis cookbook' requires more than just a simple knowledge of the reactants, conditions and products from previous synthesis attempts. Indeed, detailed information regarding each part of the process is required, both generally and specifically for differences between classes of material and

processes (*e.g.* zeolites *vs.* MOFs and clear solutions *vs.* gels). In addition, in order to ensure the information is representative of a true synthesis process at least some of these data must be obtained under challenging *in situ* chemical and physical conditions (*e.g.* high temperature and pressure) which often necessitates a 'black box' sample environment which is difficult to penetrate.

Despite these demands however, the fundamental study of the formation process of CNFMs has continued over a number of decades, utilizing many different experimental techniques and ingenious setups. Increasingly, high-brilliance synchrotron-based techniques have been used to probe these challenging systems and in this tutorial review we will discuss their role in the understanding of several classes of nanoporous materials.

2. The scale of the problem and the synthesis tool kit

A detailed discussion of the many formation mechanisms proposed for CNFMs is beyond the scope of this tutorial review and we refer the reader to works authored by Cundy and Cox,[10] Xu and Yu[11] and Ferey.[12] However, at the broadest level Fig. 1 outlines the general formation process which can be divided into five stages. (1) During **initial mixing** the source components of the synthesis are homogenized forming a solution or gel-based 'mother liquor'. Then, depending on the nature of the species in the mother liquor (2) **pre-crystalline nucleation** of 'nanoparticles' may occur which then undergo (3) **nanoparticle growth** through either agglomeration of surrounding nanoparticles or consumption of species from
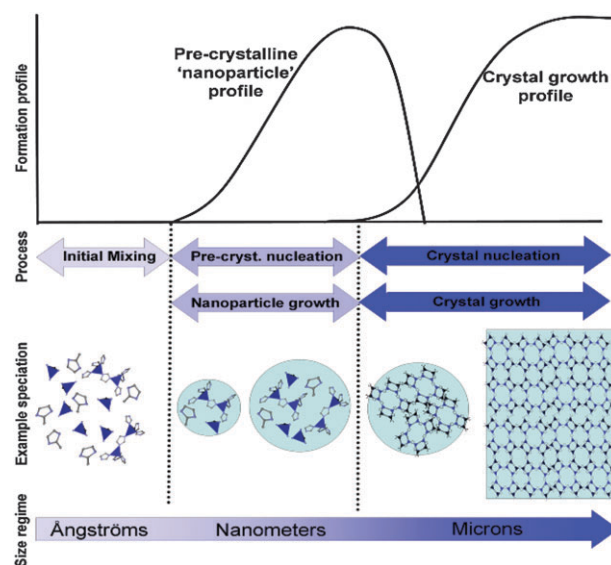
Bert Weckhuysen (42), a native Belgian, received his masters degree from Leuven University (Belgium) in 1991. After finishing his PhD studies under the supervision of Prof. R. A. Schoonheydt in 1995, he has worked as a postdoctoral fellow with Prof. I. E. Wachs at Lehigh University (USA) and with Prof. J. H. Lunsford at Texas A&M University (USA). Weckhuysen is since 2000 full professor inorganic chemistry and catalysis at Utrecht University. He has authored over 250 publications in peer-reviewed scientific journals and received several research awards, including the 2006 Gold Medal from the Royal Dutch Chemical Society, the 2007 DECHEMA Award from The Max Buchner Research Foundation (Germany) and the 2009 Netherlands Catalysis and Chemistry Award. Weckhuysen is also scientific director of the Dutch Research School for Catalysis (NIOK).

Bert M. Weckhuysen

Fig. 1 A general outline of the stages of CNFMs growth including the formation profile of nanoparticles and crystals, the processes occurring at each stage, examples of speciation and the size regime these species tend to cover. The specific example of speciation is taken from the MOF-type materials (blue triangles = framework metal, ring structures = organic linker, grey boxes = larger nanoparticles/crystallites), however the overall procedure can represent any microporous material.

Table 1 List of the techniques used to study the formation of CNFMs discussed in this tutorial review. Note that 'type' is discussed in the text, Multi. notes if the technique has been performed in a multi-technique setup to date and the reference list excludes review articles unless otherwise indicated. Finally for *in situ* environments '¹' indicates experiments that were performed at or close to ambient temperatures and pressures.

Type	Technique	Ab.	Multi.	In situ	Pseudo situ	Ex situ	Size regime	Information	Notes	Ref.
Synchrotron	Small angle X-ray scattering	SAXS	✓	✓	✓	✓	Å-µ	Amorphous particle size and shape	More correlated systems are difficult to interpret	25,26,27,29,33,34,35,36,37,38,39,40, 44,45,46,55,66,76
	Wide angle X-ray scattering	WAXS	✓	✓	✓	✓	Å-µ	Amorphous regions, intermediate and product formation and characteristics	Monochromatic source (*usually* less penetrating, higher quality)	25,26,29,34,44,45,46,55,56,61,65,66,70
	Energy dispersive X-ray diffraction	EDXRD	✓	✓	✓	✓	Å-µ	Amorphous regions, intermediate and product formation and characteristics	Polychromatic source (*usually* more penetrating, lower quality)	47,48,49,53,56,59,60
	Extended X-ray absorption fines structure	EXAFS	✓	✓	✓	✓	Å	Element specific local (bulk) information on bonding	Element specific, hard X-ray probe	55,59,65,66,70,71,73
	X-ray absorption near edge structure	XANES	✓	✓	✓	✓	Å	Element specific local (bulk) information on coordination and oxidation state	Element specific, hard X-ray probe	55,65,66,70,71
	Pair Distribution function/correlation function	PDF/CF	✓	—	✓	✓	Å-nm	Non-element specific local (bulk) order information	Requires high energy X-rays, problems with solvent signal obscuring data	46
	High energy X-ray diffraction	HEXRD	✓	✓	✓	✓	Å-µ	In principle can incorporate SAXS/WAXS and PDF information	Highly penetrating. Not widely available	16,17,46
	Scanning transmission X-ray Microscopy	STXM	—	—	✓	✓	nm	Direct imaging of particles and elemental/electronic information	Unutilized to date—few opportunities for pseudo *in situ*	review ref. 78
Combined	Raman	—	✓	✓	✓	✓	Å	Organic-inorganic interactions and organic conformation changes	Fluorescence can cause problems	55,69
	Ultra violet-Visible	UV-Vis	✓	✓	✓	✓	Å	Electronic state and local environment		55,68
	Infra-red	IR	✓	✓	✓	✓	Å	Bond formation and type	Hydrothermal systems as yet un-probed	28,31,41,46
Independent	Dynamic/static light scattering	DLS/ SLS	—	✓	✓	✓	Å-µ	Amorphous particle size and shape		18,28,35,36,37,40,42,45
	Transmission electron microscopy	TEM	—	✓[1]	✓	✓	Å	Direct imaging of species	Sample damage can occur during measurement	27,28,34,37,38,40,43,46
	Scanning electron microscopy	SEM	—	✓[1]	✓	✓	Å-nm	Direct imaging of species	Sample damage can occur during measurement	18,25,33,37,42,45,59
	Atomic force microscopy	AFM	—	✓[1]	✓	✓	Å	Imaging surface of forming species		37,75
	Small angle neutron scattering	SANS	—	✓	✓	✓	Å-µ	Amorphous particle size and shape, contrast and (with SAXS) 'core-shell' information	Large sample environments but low time resolution	35,37,39
	Nuclear magnetic resonance	NMR	—	✓	✓	✓	Å	Local (bulk) state of nuclei within system	Commonly used to identify SBUs	31,35,36,41,42,76
	X-ray diffraction	XRD	—	✓	—	✓	nm-µ	Identification of crystalline products	In principle can be used *in situ*, but data collection is usually slow	18,28,31,33,37,41,43,48,49,59,68, 69,73,74
	Gas phase chromatography	GPC	—	—	—	✓	Å	Identity of small solution species	Used to identify SBUs	40, review ref. 10
	Mass spectroscopy	MS	—	—	✓	✓	Å	Identity of small solution species	Used to identify SBUs	review ref. 10

solution. At some point during the synthesis (4) **crystal nucleation** then occurs and the growing nanometer sized particles closely resemble the final microcrystalline structure. Finally, (5) **crystal growth** of these nuclei occurs again *via* agglomeration or solution species consumption. Of course, this simplified picture does not encompass the vast array of species (*e.g.* clear solutions zeolites form from monomeric/polymeric species,[10] whilst MOFs can form from larger 'building units',[12] skipping the initial stages) and the interactions which may occur (*e.g.* the amount of structural ordering and the onset of stage 3). However it does demonstrate the scale of the problem we are faced with. To fully understand the nanoporous formation process information must be obtained over length scales of several orders of magnitude (as with other fields such as heterogeneous catalysis[13]), from Ångström sized pre-nucleation species to nanometer sized particles and to the final micron sized crystalline materials. At each stage the local electrostatic, conformational and chemical interactions and global particles sizes, shape and distributions (both for the organic and inorganic species) must then be obtained.

In addition, this information must be obtained under conditions as close to 'real' as possible. Indeed, whilst *ex situ* and pseudo *in situ* experiments provide high quality data, they require either complete removal from or quenching of the synthesis environment, which can affect the delicate balance of species in solution and make the data difficult to relate to the true operational conditions. Fully *in situ* experiments overcome this problem, providing detailed temporal information on the sample in its 'natural' condition, although this can sometimes be at the expense of data quality.

To obtain a complete understanding of this complex process therefore requires numerous techniques and, in Table 1, we highlight those discussed in this tutorial review. It is divided into three sections, *synchrotron*-based techniques, those which have to date been *combined* with synchrotron-based techniques and *independent* techniques not performed in combination with synchrotron techniques but utilized in a complementary manner (note that it is of course possible to perform many of the synchrotron-based techniques in a lab but with very slow acquisition times). Together these form the 'tool kit' required to investigate the formation process outlined in Fig. 1 and it is clear that it is not only synchrotron-based techniques that can be performed *in situ*. Indeed, depending on the conditions required for synthesis, DLS, NMR and even TEM, can to some extent be performed in this manner, however it is the high brilliance and flux of the synchrotron-based techniques that provide the penetration to probe the widest range of sample environments with good time resolution and without compromising data quality. As a consequence the flexibility of the sample environment allows some synchrotron techniques to be 'combined' with the spectroscopic techniques in Table 1 to provide complementary and coherent information over large parts of the formation mechanism.

Thus, the synchrotron-based technique (and combined multi-technique studies) can reveal detailed accurate and complementary information under fully *in situ* conditions which cannot be *easily* obtained from techniques with lower sample penetration and/or less realistic sample environments.

However, as will be demonstrated in the examples below, it is essential to remember that whilst synchrotron techniques may often provide the 'backbone' of information on the formation of a particular system it is often the highly detailed complementary but independently obtained information that 'fleshes out' the mechanism fully and thus, it is a combination of synchrotron and non-synchrotron techniques which may ultimately rationalize the formation process of CNFMs.

3. Penetrating the black box

To perform any experiment *in situ* it is essential that the experimental cell allows the penetration of the synthesis 'black box'[14] by the desired technique(s) whilst maintaining the conditions usually used to synthesize the material as much as possible. Under mild conditions (*e.g.* room temperature synthesis) the cell can be flexibly designed around the technique of choice, allowing for example TEM and SEM to be performed '*in situ*' (Table 1) with no trade off between realistic *in situ* conditions and high quality data with a good time resolution. More usually however, elevated temperatures and pressures are required and there is therefore a trade off as the cell must be able to withstand the more harsh conditions but still allow penetration of the measurement probes. In the case of synchrotron-based techniques that usually employ transmission geometries it is the flux and energy of incident X-rays that determine the ability of the cell to approach the most challenging conditions, whilst for experiments which combine spectroscopic techniques such as UV-Vis or Raman, the cell must either contain windows or be constructed from a material transparent to the appropriate wavelengths, which can of course then affect cell integrity.

For synchrotron-based transmission techniques the two most commonly utilized cells are given in Fig. 2, and have
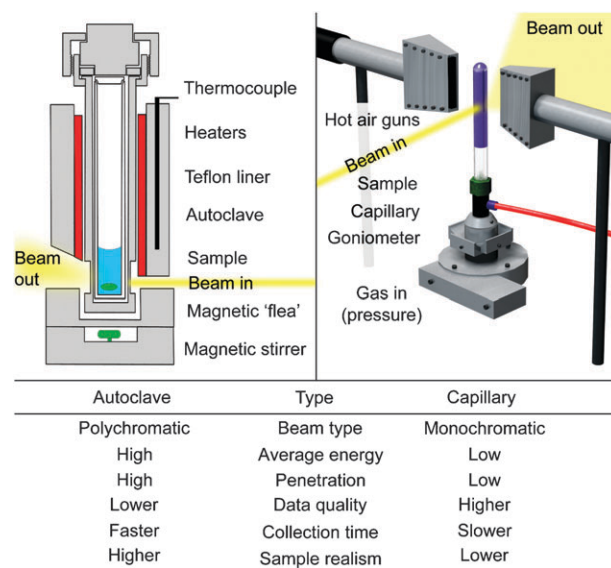

Autoclave	Type	Capillary
Polychromatic	Beam type	Monochromatic
High	Average energy	Low
High	Penetration	Low
Lower	Data quality	Higher
Faster	Collection time	Slower
Higher	Sample realism	Lower

Fig. 2 The most commonly utilised cells for synchrotron transmission studies with remarks regarding the usually used beam type, 'average' energy and penetration ability and the data quality, collection time and sample realism associated with this. Each variable is dependent on the beamline, the sample environment and the other variables. For example for the same beam and cell a faster collection time can result in lower data quality.

been described in more detail by Norby.[15] Here the large autoclave sample environment can obtain a wide range of realistic conditions as it can cope with most extremes of temperature and pressure required for hydrothermal CNFM synthesis. Its robust construction means however that only synchrotron setups with a very high energy range and flux can penetrate. Thus, it is most commonly employed on 'White' energy dispersive (ED) beamlines. Unfortunately, whilst very penetrating, the quality of ED data is not always high and there is therefore often a preference for using monochromatic setups (which also allow element specific techniques such as X-ray absorption spectroscopy (XAS)). Unfortunately, these are then usually located on far less penetrating bending magnet beamlines (generally <30 KeV). This of course then results in a compromise in cell design to acquire good data with a reasonable time resolution, which in turn reduces the realism of the system somewhat. The capillary type cell demonstrated in Fig. 2 is a good example of this and these type of cells are particularly important as they also allow the aforementioned use of spectroscopic techniques such as Raman and UV-Vis. Other cells used include compressed mica window systems and stop flow cells.

More recently, some studies have demonstrated the utilization of (increasingly available) very high energy monochromatic beamlines[16,17] which allow high quality data to be obtained from autoclave-like sample environments, potentially negating the need for compromises between cell design and experimental measurement conditions.

4. Zeolite clear solution studies

CNFMs can be formed from numerous mother liquors including dense gels, clear solutions and even solid mixtures (i.e. steam assisted conversions). Clear solutions containing colloidal or sub colloidal particles represent 'models' as they allow both a wide variety of techniques to be used (e.g. DLS), which cannot be utilized on thick gels and a (potentially) simplified analysis. To date the most common inorganic materials synthesized from clear solutions are zeolites (e.g. Schoeman et al.[18] and Cundy and Cox[19]), which consist of a framework of silicon and/or aluminium metal centres bridged by oxygen atoms (for details on different nanoporous structures we refer the reader to the book of Wright[20]).

4.1 SAXS/WAXS combination

Silicalite-1 (framework code MFI[21]) and zeolite A (LTA) are the most extensively studied zeolites, with the combination of synchrotron-based SAXS and WAXS regularly utilized. Essentially, both techniques are a result of in-phase scattering of X-rays by electrons à la Bragg's law. For a complete theory of scattering and diffraction we recommend Glatter and Kratky[22] (freely available online), Svergun and Koch[23] and Clegg et al.[24] As the angle at which X-rays are coherently scattered is inversely related to the distance between the scattering electrons (i.e. $1/d$) SAXS/WAXS provides a powerful tool for the examination of both the overall diameter of globally microcrystalline/amorphous particles (SAXS) and larger crystalline entities, where scattering occurs primarily from the very small lattice d-spacings between atomic planes

(resulting in sharp diffraction peaks at well defined positions in the WAXS). Thus the techniques can cover the formation process from the early stages of nanoparticle growth (nanometers) to the late stages of crystallization (microns).

One of the most widely known series of works to use this powerful combination is that of De Moor et al.[25,26] where the evolution of silicalite-1 was monitored in situ and several particle species were observed. An example of the SAXS data obtained from one such study is given on the left in Fig. 3,[25] whilst on the right the intensity of each species as a function of time is plotted. Using a direct relation between the scattering vector (q) at which the broad intensities were observed and the d-spacing ($q = 2\pi/d$) De Moor et al.[25,26] determined the size of these particles and described them as primary units (ca. 2.8 nm), aggregates (ca. 10–15 nm) and larger crystallites (at very low q). Bragg scattering was then observed either in the WAXS or, depending on the detector distance, the SAXS camera. The observation of two non-crystalline nanometer sized particle distributions during zeolite synthesis was important, but was not new to this work. Indeed, Regev et al.[27] previously used complementary cryo-TEM and quenched SAXS to observe similar 5 nm and 22 × 8 nm cylindrical species under pseudo in situ conditions, whilst Schoeman and others[28] have also demonstrated the ability of DLS to observe such particles.

These SAXS/WAXS measurements did however for the first time allow the formation of these particles to be observed dynamically, over a very large size range (4 orders of magnitude, 0.17–6000 nm) and under truly in situ conditions. The experiments therefore not only confirmed the previous pseudo in situ observations under conditions relevant to synthesis (i.e. where weak silicalite-organic interactions are intact) but also provided essential information on how these nanometer particles evolved in relation to crystal formation (not directly observable by light scattering techniques alone). For example, it was shown that the primary units were unaffected by factors such as the alkalinity of the solution and remained almost unchanged in intensity during aggregate formation (Fig. 3) but where consumed during crystallization.
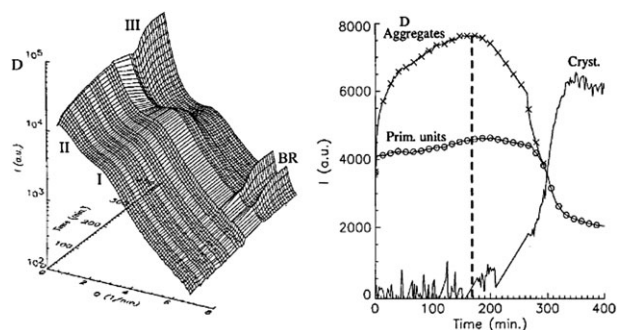

Fig. 3 Example SAXS data obtained by De Moor et al. during the synthesis of clear solution silicalite-1, where I = primary units, II = secondary units, III = SAXS crystallites and BR = Bragg reflections (left) and the measurement of the intensity of some of these features as a function of time (right). Reprinted in part with permission from P. de Moor, T. P. M. Beelen, R. A. van Santen, L. W. Beck and M. E. Davis, J. Phys. Chem. B, 2000, **104**, 7600–7611. Copyright 2000 American Chemical Society.
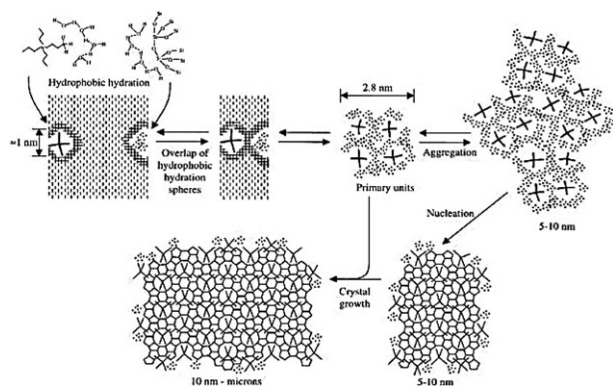
Fig. 4 The silicalite-1 formation mechanism proposed by De Moor *et al.* incorporating primary units and nano-sized aggregates Figure from P. de Moor, T. P. M. Beelen, B. U. Komanschek, L. W. Beck, P. Wagner, M. E. Davis and R. A. van Santen, *Chem.–Eur. J.*, 1999, **5**, 2083–2088. Copyright Wiley-VCH Verlag GmbH & Co. KGaA. Reproduced with permission.

On the other hand, the aggregates were observed to increase in intensity during the initial stage of reaction and were then rapidly consumed during crystal growth.

From several *in situ* time-resolved experiments De Moor *et al.* derived the formation mechanism given in Fig. 4.[26] Here primary units are formed from the solution, which then aggregate and, with internal re-ordering, evolve into crystalline materials which continue to grow through primary unit addition. In addition we note that the SAXS data also exhibited some fractal-like characteristics and, although not explicitly included in the mechanism outlined in Fig. 4, a modification by Beelen and van Santen[29] has also described the aggregation as fractal-like (although we note that Sankar and Bras[30] have discussed the problem of over-interpretation of the data with respect to this). The mechanism in Fig. 4 not only incorporated the ideas from previous studies (*e.g.* the interaction of small silicalite and organic units as observed by Burkett and Davis[31]) but also for the first time indicated the importance of larger colloidal species in the formation process, as suggested by theoretical Derjaguin-Landau-Verwey-Overbeek (DLVO) interaction calculations.[32] These initial SAXS/WAXS studies therefore greatly contributed to 'the emergence of the colloid' in zeolite synthesis.[19]

Interestingly, we note that, unlike other fields such as protein crystallography[23] no more complex analysis of the SAXS data (*e.g.* accurate particle size determination *via* Guinier analysis[22] at low q or particle size and shape determination from form factor modelling at mid q) was provided. Some authors have attempted this (*e.g.* Cheng *et al.*[33] and Fan *et al.*[34]), however the correct application of such procedures relies on there being highly dispersed non-interacting solutions of mono-dispersed particles. Therefore, whilst in their initial state clear solutions may confirm to this special case, once synthesis proceeds considerable inter-particle correlations must occur and the system is often poly-dispersed. Then, as discussed by Svergun,[23] SAXS alone cannot be used to construct the individual components of the system and the amount of useful information that can be obtained from the technique relies on the acquisition of suitable complementary information.[23]

This is exemplified by Aerts *et al.*[35] who demonstrated that the exact size of the nanoparticle is not accurately determined by the $q = 2\pi/d$ relation as it does not take into account polydispersed inter-particle interactions. Of course, performing a simple sample dilution to remove these interactions would significantly alter the highly correlated system and considerably affect the species under observation. Instead therefore, the group utilized quantitative NMR to determine the volume fraction of the sample and included this in the calculation of the SAXS particle size. The resulting SAXS-NMR size determination was more accurate than from SAXS alone, although it did still rely on some assumptions. This particular work nicely demonstrates the potential advantage in utilizing complementary pseudo *in situ* and/or *ex situ* techniques to support and understand *in situ* synchrotron-based data.

4.2 Complementary silicalite-1 studies and the nature of nanoparticle formation

A series of studies combining several techniques in a single work (but not always in a single experiment) to obtain a more detailed understanding of the clear solution formation process and the nature of the nanoparticle, resulted in three opposing mechanisms, recently summarized by Aerts *et al.*[36] and reproduced in Fig. 5. They differ in the species that are responsible for growth, the extent of zeolitic ordering in the nanoparticles and the involvement of smaller species during the aggregation steps.

In the first scheme the zeolitic framework develops only after nanoparticle aggregation, through internal reordering. Nanoparticle and crystal growth then occurs *via* addition of either elementary particles or primary units. This mechanism is effectively that described in the work of De Moor *et al.*[25,26]
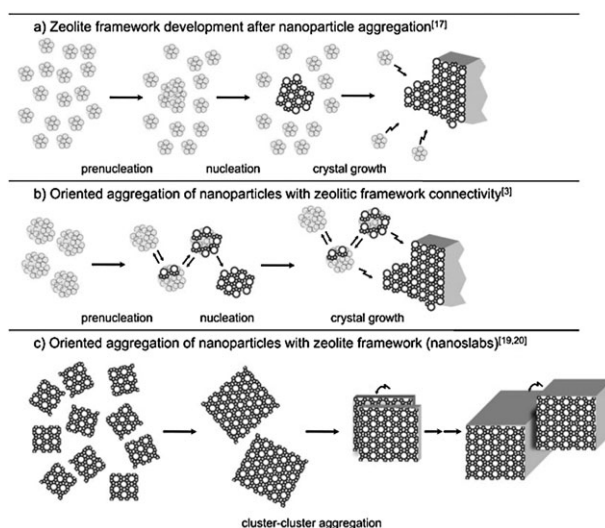

Fig. 5 The three schemes for zeolite growth as described by Aerts *et al.* Particles with poorly developed framework connectivity are in light gray; zones with zeolitic framework connectivity are depicted in dark gray; the zigzag arrows indicate an aggregation event. Figure from A. Aerts, M. Haouas, T. P. Caremans, L. R. A. Follens, T. S. van Erp, F. Taulelle, J. Vermant, J. A. Martens and C. E. A. Kirschhock, *Chem.–Eur. J.*, 2010, **16**, 2764–2774. Copyright Wiley-VCH Verlag GmbH & Co. KGaA. Reproduced with permission.

This journal is © The Royal Society of Chemistry 2010

and Doktor *et al.*[29] The second scheme describes an 'aggregative growth' mechanism proposed by the group of Tsapatsis (*e.g.* Davis *et al.*[37]) as a result of an in-depth room temperature formation study of silicalite-1 (allowing TEM and AFM to be performed '*in situ*'). Here only large aggregates (no primary particles) were observed by SAXS and interestingly, along with cryo-TEM and AFM data it was shown that, whilst these nanoparticles did not grow for long periods of time, they did continue to evolve with regard to their colloidal stability. *In situ* TEM also demonstrated that some of the forming crystals had an aggregate-like morphology. This leads to a mechanism where, after their initial formation from solution, the nanoparticles undergo a series of ordering steps and become increasingly more zeolite-like. The most ordered of these then contribute to crystal growth through aggregate addition. The initial study proposed that these nuclei were considerably ordered. However, a subsequent cryo-TEM study[38] later indicated that some ordering must continue later into the formation process.

In addition, based on previous studies by Fedeyko *et al.*,[40] this work also shows the potential of combining neutron and X-ray studies. The SAXS results gave a smaller apparent particle size compared to small angle neutron scattering (SANS), demonstrating that the structure of these nanoparticles can be described as consisting of a 'core' of silicate and 'shell' of organic template (weakly scattered by X-rays and therefore unobserved in the SAXS).

In both the above schemes the initially nanoparticle bared no resemblance to the final nanoporous product. The final scheme in Fig. 5, however, proposes a nanoparticle with considerable zeolite-like connectivity at all stages of growth. This 'nanoslab' aggregation was proposed by Kirschhock and coworkers[40] from a series of complementary *in situ* and *ex situ* studies under specific high TPA/silicate ratios and mild post synthesis conditions. Here initial precursor species, similar to those of Burkett and Davis,[41] were observed by NMR, scattering and GPC. A Porod analysis of the SAXS data revealed the presence of 'nanoplates' formed from the addition of several zeolitically ordered nanoslabs. The stepwise aggregation of these materials from slabs to tablets and the final crystal was then observed by DLS, whilst cryo-TEM imaging was used to provide evidence of their structured nature. More recently, a 'hybrid' mechanism has been proposed by Aerts *et al.*[36] where the initial particles become either poorly or highly ordered during the initial mixing. The more highly ordered species then take part in the nucleation processes. Oriented aggregation of the formed 6 nm particles (rather than cluster-cluster aggregation) then allows the growth of the final crystalline product.

4.3 Comparison with zeolite A synthesis

In the previous sections we have described the formation of silicalite-1 from clear solution. Similar studies have also been performed on other zeolite systems such as zeolite A and, as with silicalite-1, these were initially non-synchrotron based. For example, the SEM/SLS study of Gora *et al.*[42] demonstrated the formation of crystalline regions within amorphous nanoparticles, whilst the remarkable TEM images of

Mintova *et al.*[43] directly visualized this amorphous to crystalline transition. The use of non-synchrotron based techniques was facilitated by the fact that zeolite A can be synthesized at room temperature over several months allowing '*in situ*' measurement, however as with silicalite-1, these studies cannot easily explore all of the complex interactions or cover the size range within the system. For example, the TEM results of Mintova *et al.*[43] can be described by either Scheme 1 or 2 in Fig. 5. Non-synchrotron based techniques also cannot examine the effects of elevated temperature and pressure that are more usually associated with zeolite synthesis.

Again therefore, time resolved synchrotron measurements (often in combination with other techniques) have been used to more fully describe the system. Grizzetti *et al.*[44] for example utilized the SAXS/WAXS combination to identify two independent populations of particles and describe a mechanism broadly similar to De Moor *et al.*,[25,26] whilst Fan *et al.*[34] observed similar nanometer-sized entities and structure in the SAXS data. Here the data could be fitted to a cubic form factor which suggested a relatively homogenous solution of nanoparticles.

More recently, O'Brien *et al.*[45] have performed a series of *in situ* and *ex situ* measurements (SAXS/WAXS, DLS and SEM) on the zeolite A system. Like the group of Tsapatsis,[37,38] this research team did not observe any primary particles; however the size of the nanoparticles did increase as a function of time (confirmed by both DLS and SAXS). This then suggested a similar mechanism, but with some involvement of smaller species. To investigate this further the group utilized a time resolved invariant type analysis (for a 2 phase system) of the SAXS curve:

$$Q = \int_0^\infty q^2 I(q)\,\mathrm{d}q = \langle n_e \rangle^2 \varphi_1 \varphi_2$$

Here the invariant Q can be calculated by measuring the integrated intensity (I) of an I *versus* $q^2 I$ plot (where q is the scattering vector) of the entire SAXS pattern. This value, although 'invariant' with regard to nanoparticle size and shape, is proportional to the electron density difference between the phases within the system ($\langle n_e \rangle^2$) and the volume fractions of these (φ_i). It is therefore sensitive to the total amount of scattering observed by the camera.

As shown in Fig. 6, it was demonstrated that the invariant increased most rapidly during the period of most rapid growth of the nanoparticles both in terms of their diameter and number of scatterers (*i.e.* intensity increase). This strongly indicated that nanoparticle growth occurred *via* the addition of small solution species beyond the range of the SAXS camera. The study therefore demonstrates the usefulness of this type of analysis in extracting additional information from the SAXS curve, although we must note that for accuracy extrapolation to infinity at low q and 0 at high q (not performed in this study) should be considered (see Glatter and Kratky[22]).

4.4 Towards a unified mechanism?

From the examples of silicalite-1 and zeolite A it is clear that *in situ* time resolved synchrotron studies have played a pivotal
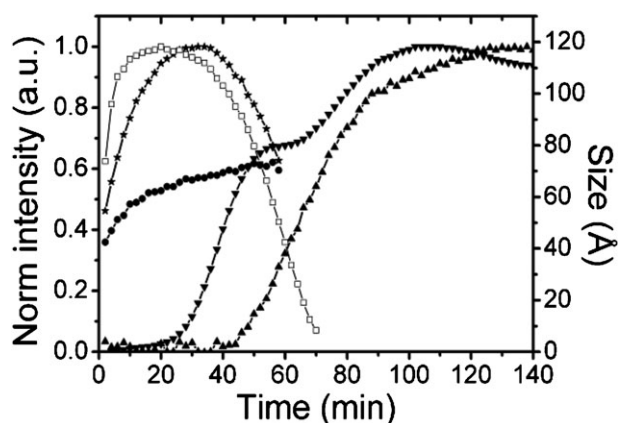
Fig. 6 Intensity plots taken from SAXS/WAXS data during the formation of zeolite A from clear solution. The most rapid increase in the invariant (– □ –) occurred as the number (–★–) and size of nanoparticle increased (–●–) increased most rapidly. Here the crystallite feature in the SAXS (–▼–) and Bragg scattering in the WAXS (–▲–) are also given. Reprinted with permission from M. G. O'Brien, A. M. Beale, B. W. M. Kuipers, B. H. Erne, D. W. Lewis and C. R. A. Catlow, *J. Phys. Chem. C*, 2009, **113**, 18614–18622. Copyright 2009 American Chemical Society.

role in understanding the species present during the formation of zeolites from clear solution. They have not only demonstrated that nanoparticles form under fully in situ conditions but have also been able to observe the interaction between each species and the formation of crystalline materials in a dynamic manner. The studies do however also show that the interpretation of the results has been most effective when combined with other independent measurements from the synthesis 'tool kit' described in Table 1.

Interestingly, however, despite this vast amount of work we note that even for a single 'model' system there remains little consensus on which of the proposed mechanisms is most likely (*e.g.* Fig. 5). This highlights the complexity of the CNFMs formation processes and indicates that even for a single structural framework the exact synthesis mechanism may differ significantly depending on the synthesis conditions. It seems apparent then that there is a need to compare and contrast different synthesis mixtures that form the same material but as a result of different formation species. Essential to this will be the ability to examine each system under (as much as possible) the same conditions and with the same combination of techniques. In this regard, multi-technique synchrotron-based experiments can more easily facilitate this, whilst the recent combination of synchrotron and non-synchrotron techniques (to date used only to study AlPOs, see below) would appear to offer the opportunity to compare these in a complementary fashion and begin to identify a 'mechanistic set' for different formation conditions.

4.5 Germanium, secondary building units and other techniques

Another way to obtain more insight into the formation process is to deliberately vary one synthesis parameter (*e.g.* chemical composition) and observe any resulting effects. Recently, this concept was used to examine metal (specifically germanium) substitution into the structural framework of both silicalite

and zeolite A. For example, using the SAXS/WAXS combination Cheng *et al.*[33] observed acceleration in the rate of crystallization of Ge-Silicalite-1 up to a Si/Ge ratio of 15–25 (although interestingly a decrease was noted on further substitution), whilst O'Brien *et al.*[45] observed a similar effect in zeolite A, along with an increase the size the nanoparticles and variations in the morphology of the final product. These studies demonstrate that small variations in the synthesis conditions can significantly alter the formation mechanism. In zeolite A, Ge substitution appears to affect the entire formation process from aggregate nucleation to crystal growth. The origin of this 'promotion effect' may be a stabilization of particular T-O-T (where T is Si, Al or Ge) angles within the growing aggregates, allowing the formation of specific secondary building units (SBUs), such as double 4-membered rings.

Like the nature of the nanoparticle, the role of such SBUs within the formation process of CNFMs (either within the nanoparticle or solution) remains under considerable debate. This review does not specifically detail the numerous non-synchrotron-based studies (*e.g.* NMR and MS) that have contributed to this area and we refer the reader to the review of Cundy and Cox,[10] however it is important to note that probing the evolution of these specific Å-sized species in situ and in relation to the wider changes within the solution (or gel) remains a challenge which must be resolved to entirely understand the formation process.

With respect to this, combined multiple technique setups may again be of considerable use as they can for example 'probe' the substituted elements environment (XAFS) and combine this data with that obtained from the evolving nanoparticles (SAXS) and (through Rietveld analysis) the location of the substituted atoms within the forming framework (WAXS, with some improvement in detector resolution). Such setups may therefore be able to provide a complete overview of the formation process from including both nanoparticle and SBUs.

In addition, HEXRD measurements over large wave vectors can not only provide WAXS (and potentially SAXS) data on the system but also, through a PDF/CF analysis of the amorphous scattering data, details on the interactions between elements on the Å level. The results are similar to EXAFS, but do not require a target molecule to be inserted into the system. To date the work of Fan *et al.*[46] represents the only example of this in the field of nanoporous materials, with correlations associated with medium range order within the nanoparticles identified during the formation of a zeolite A solution where primary particles were also identified. As demonstrated in Fig. 7 these correlations were interpreted as being due to 4 and 6-membered ring species in the solution prior to heating. Unfortunately, the strong oxygen interactions (O–O) from water in the system limited these measurements to *ex situ* studies. However, this technique may still prove to be particularly useful in examining non-aqueous CNFMs synthesis, such as ionic liquid formed AlPOs or MOFs where such interactions would be minimized.

5. Aluminophosphate gel studies

In cases where a clear solution is not used for the synthesis of a CNFM, the analytical challenges from techniques such as
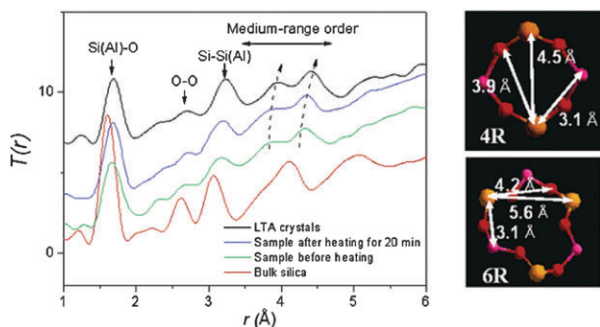
Fig. 7 The HEXRD correlation function technique as demonstrated by Fan *et al.* allowed the determination of medium range order and the identify of SBUs both within the initial gel and the forming nanoparticles of zeolite A. A 4MR and 6MR with various distances between the atoms are shown (right) for comparison (Yellow = Si, pink ball = Al and red = O). Reprinted with permission from W. Fan, M. Ogura, G. Sankar and T. Okubo, *Chem. Mater.*, 2007, **19**, 1906–1917. Copyright 2007 American Chemical Society.

SAXS become even greater due to increased inter-particle correlations. However, as many CNFMs cannot be synthesized from model clear solutions, other synchrotron-based measurement procedures have been developed to cope with this. In previous decades the focus has been on obtaining information from either the WAXS data alone or combined with EXAFS, although more recently some groups have also combined SAXS and spectroscopic measurements to allow direct correlation of several data streams and overcome some of the difficulties dealing with the dense gel.

5.1 WAXS, intermediates and the crystallization curve

Although an analysis of the crystallization curve alone cannot provide a complete or conclusive interpretation of the nucleation and growth mechanism, direct examination of this part of the growth process and analysis of this with several analytical models can provide some useful indications. Note that here we discuss these procedures with regard to gels, however they are of course equally valid (and have been used) in the study of clear solution WAXS data.

In the first examination of an AlPO system with EDXRD He *et al.*[47] demonstrated from a direct examination of the crystallization profile that VPI-5 had a surprisingly short induction period, concluding that the nucleation event may take place during an aging step of the gel. Walton *et al.*[48] have also observed 'pauses' in the crystallization curve during the formation of zeolite A from a gel and it was proposed that this was due to a periodic release of nuclei from the inhomogeneous gel (although recently[45] similar pauses have been noted in a clear solution zeolite A synthesis, indicating this change may be due to some other process).

Measurement of the scattering throughout the formation process also allows intermediates to be observed, which can then be either directly identified or isolated by quenching for detailed *ex situ* examination. For example, Loiseau *et al.*[49] observed intermediates during the formation of ALPO MIL-57 which, after isolation and examination by single crystal techniques, were determined to be chain-like in nature. These

species were suggested to play a significant role (along with interaction with sodium) in the formation of the final product. Similar chain-like intermediates have also been isolated for other systems including the ULM gallophosphates (*e.g.* Millange *et al.*[46]) lending weight to the argument that the formation processes of nanoporous phosphate materials from a gel may differ somewhat from zeolite systems, with the formation of more chain-like structural units. Such a mechanism has been proposed for AlPO formation by Oliver *et al.*[50] and is described in more detail in a recent review by Yu and Xu.[11]

5.2 Peak profiling and additional information

Aside from 'direct' information, fitting the growing diffraction peaks with appropriate functions (*e.g.* Gaussian) allows the intensity, area and full width at half maximum (FWHM) to be obtained, from which additional details on the formation process can be derived.

For example, as smaller crystallites expose fewer lattice planes to the X-ray beam, (for a detailed derivation of this phenomenon see Guinier[51] and Patterson[52]) a measurement of the FWHM ($\beta_{2\theta}$) of a peak can allow the determination of particle size (*d*) in that particular crystallographic direction (between 10–1000 Å) *via* the Scherrer equation:

$$d = \frac{K\lambda}{\beta_{2\theta}\cos\theta_0}$$

(*K* depends on the particle form, although 0.939 is commonly used).

Accurate determination relies on both on high quality data (low noise, particularly at the initial stages of Bragg peak formation) and a good knowledge of the instrumental broadening, which is not always possible with *in situ* synchrotron based setups. The technique has therefore been more usually employed to demonstrate relative changes in crystallite size (*e.g.* the unsurprising increase in zeolite crystal domains as crystallization proceeds[54]), although Grandjean *et al.*[55] have quoted the size of CoAPO-5 to vary from 40–65 nm during formation. In addition, it is important to note that the application of this equation may not always be suitable. For example, Schlenker and Peterson[53] have indicated that for very small crystallites (of a few unit cells) the Scherrer equation does not hold, whilst Chiche *et al.*[54] have demonstrated that the Debye formula may be of more use for nanosized materials.

A simpler overlay of the curves obtained from several peaks related to different crystal planes can also be used directly to obtain basic information regarding the dimensionality of the growing crystals. For example, the growth of ULM-5 was determined by Francis *et al.*[57] to be isotropic, with each curve having a very similar profile. References within that work then demonstrate the effect of non-isotropic growth on these profiles.

5.3 Modelling and kinetics

To obtain underlying kinetic detail on the growth of AlPOs a variety of models have been employed, although the complexity of the system makes a full analytical understanding of

the process difficult. Most commonly used the Avrami and Erofe'ev model *via* a Hancock–Sharp analysis[58] of the crystallization curve:

$$\ln[-\ln(1 - \alpha)] = n \ln(t) + n \ln k$$

where α is the extent of the reaction (the ratio of intensity at each point compared to the final intensity) and t is the time from the start of crystallization. The entire process is demonstrated schematically in Fig. 8 for the synthesis of CoAPO-36. Here fitting the initial data reveals the expected crystallization curve and a $\ln[-\ln(1 - \alpha)]$ *vs.* $\ln(t)$ plot of this (typically between $\alpha = 0.15$ to 0.8) then gives a linear region from which the reaction rate (k) and the constant n can be determined. If k is then obtained over several reaction temperatures the Arrhenius expression can be used to calculate the activation energy (E_a) for the crystallization. In addition, from Hulbert,[59] n can be used to reveal information regarding the dimensionality, type of growth and nucleation of the crystallization process, as demonstrated from the reproduction in Table 2.

This analysis process has been described in more detail elsewhere[60] and has been used to derive formation information from all types of forming systems including other CNFMs such as zeolites[48] and MOFs.[61]
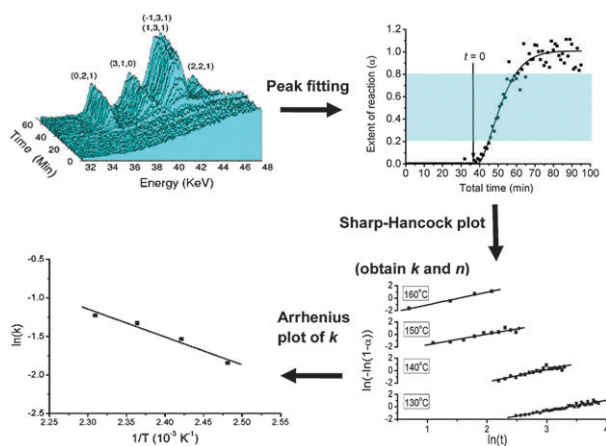

Fig. 8 Schematic of the Avrami analysis process for the formation of CoAPO-36 from initial fitting to obtaining n and k at several temperatures using the Sharp-Hancock expression to finally obtaining the activation energy through an Arrhenius plot.

Unfortunately, whilst frequently used, both the Avrami and Erofe'ev model and Hulbert's values may not actually be the most appropriate for examining most CNFM crystallization profiles. For example, it is immediately obvious from Table 2 that there is considerable overlap in n for different dimensionalities and growth types, leading to problems in definitive analysis. O'Brien *et al.*[60] for instance obtained n values indicating 1-dimensional diffusion controlled growth for CoAPO-36 in most cases but with some values being closer to 3-dimensional. Ultimately, SEM images were required to fully explain this, demonstrating that partial aggregation of 1-dimensional crystals into 3-dimensional spheres occurred in some circumstances.

More concerning however is the fact whilst the Avrami and Erofe'ev model provides a good fit of the kinetic curves and can be used for the calculation of the apparent activation energies, it essentially describes solid state reactions and not solution-mediated processes.[62] The same is true when interpreting dimensionality and growth from Hulbert's values as these were originally derived to describe solid state reactions of ceramic mixes.

Alternative curve fitting models are available and have been discussed in detail in the review of Thomson and Dyer.[63] This work, whilst rather old, contains many proposed models for understanding CNFM formation including empirical, reaction engineering, population balance and the Avrami model. It also details the advantages and disadvantages of each and discusses the prospect of combinational approaches. Thompson and Dyer[64] have also demonstrated that a modified population balance model was capable of modelling all but one of experimental curves observed at the time of publication. The more recent work of Gualtierri *et al.*[62] describes the use of a reduced form of the population model (see references therein) to examine the formation of zeolite A from clays. Here nucleation was assumed to be continuous (autocatalytic), allowing the mass fraction (m_z) of zeolite crystallized up to time (t_c) to be calculated from the simple equation:

$$M_z(t_c) = K \cdot t_c^{\,q}$$

where q describes the nucleation mechanism, with $q = 3$ representing heterogeneous nucleation and $q = 4$ homogeneous. Although a more complex expression (given in the publication) can be used to describe the system if there is a combination of heterogeneous and homogeneous nucleation, Gualtierri *et al.*[62] compared both the reduced population balance and

Table 2 Reproduction of the range of n values derived by Hulbert describing the formation process of solid-state reactions. Reproduced from S. F. Hulbert, *Journal of the British Ceramic Society*, 1969, **6**, 11

	Phase boundary controlled	Diffusion controlled
3-D (*i.e.* spheres)		
(a) Constant nucleation	4	2.5
(b) Zero nucleation	3	1.5
(c) Decreasing nucleation	3–4	1.5–2.5
2-D (*i.e.* plates)		
(a) Constant nucleation	3	2
(b) Zero nucleation	2	1
(c) Decreasing nucleation	2–3	1–2
1-D (*i.e.* rods)		
(a) Constant nucleation	2	0.5
(b) Zero nucleation	1	0.5
(c) Decreasing nucleation	1–2	0.5–1.5

the Avrami model. They demonstrated that, for the zeolite A system under study, q tended to be larger than 4, indicating (at least initially) homogeneous nucleation is occurring and that the reduced model is therefore most appropriate.

The different models described above reveal two important points with regard to this type of analysis. The first is that whilst a model may be commonly utilized in the literature to examine a particular formation process, it may not be applicable to all crystallisation processes and several models should be examined and the most appropriate chosen. The second is that more work is clearly required to examine under which conditions each of the current models applied to CNFM synthesis are actually valid. For example, as the Avrami analysis was derived for solid state reactions it may be suitable for very thick or dry gel systems but not more liquid clear solutions or MOF systems. Without such studies it remains difficult to derive much confidence in values obtained from these models, particularly when comparing the formation processes of several different materials.

5.4 Combined technique gel studies

In order to obtain more information from AlPO synthesis gels several groups have combined both synchrotron-based and spectroscopic-based techniques along with WAXS. The earliest of these combined XAS (*i.e.* EXAFS and XANES) with WAXS to obtain both local and long range order. Although such setups had been previously used to examine changes in for example catalytic systems (*e.g.* Thomas and Sankar[65]), Sankar *et al.*[66] first demonstrated their use for elucidating the formation mechanism of CNFMs. Using a capillary reactor mounted in a furnace with appropriate apertures for the X-rays, the formation of CoAPO-5 from a gel was measured, with the XAS revealing changes in the XANES region prior to crystallization. Here the pre-edge peak (1s $\rightarrow$ 3d) increased and the 'white line' absorption peak decreased in intensity indicating the conversion of the cobalt from octahedral to the tetrahedral geometry adopted in the final crystalline structure occurred prior to crystallization. EXAFS fits supported this with a reduction in the coordination number and bond distances around the cobalt also occurring.

A decade later the Weckhuysen group re-examined this synthesis with Grandjean *et al.*[56] utilizing advances in detector and reactor technology to obtain high quality XAS, SAXS/WAXS and useful UV-Vis and Raman spectroscopy in a single study utilizing the same cell to maintain similar reaction conditions. The basic experimental setup is demonstrated in Fig. 9 (with examples of the data recorded separately by Grandjean) and, as demonstrated by Beale *et al.*,[67] the cell and setup is flexible enough to allow these measurements to be performed in a single combined experiment. Here the XANES underwent similar changes to Sankar *et al.*,[66] however a detailed analysis of the high quality XAS data revealed more complex variations in the Fourier transform of the EXAFS. This demonstrated that, whilst the cobalt in the initial gel existed as octahedral Co^{2+} hexa-aquo species, these became bound *via* a Co–O–P bond to the disordered Al–O–P network before tetrahedral conversion. A slow and continuous conversion
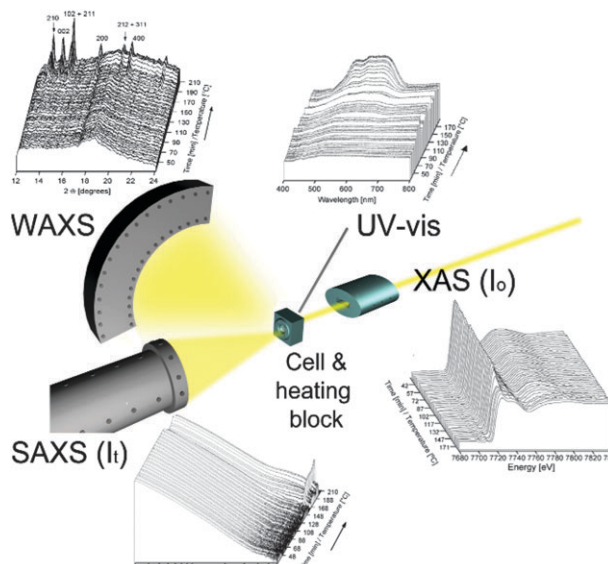

Fig. 9 The multiple technique *in situ* setup described by Beale *et al.* (ref. 67) incorporating SAXS/WAXS/EXAFS and UV-Vis. The XAS data is derived from I_o and I_t (mounted inside SAXS tube). Time resolved stack plots of data obtained separately by Grandjean *et al.* for the formation of CoAPO-5 are given as an example of the quality of data that can be obtained. Data Reprinted in part with permission from D. Grandjean, A. M. Beale, A. V. Petukhov and B. M. Weckhuysen, *J. Am. Chem. Soc.*, 2005, **127**, 14454–14465. Copyright 2005 American Chemical Society.

to the tetrahedral geometry then occurred (up to $\sim 57\%$) until crystallization was observed in the WAXS, at which time the conversion went rapidly to completion. Unlike clear solutions the SAXS (recorded sequentially with the XANES) of the thick gel resulted in no clear shoulder or maxima. However, by subtracting the power law decay dependencies (observed to be -3 over the data) broad maxima were revealed which (like de Moor and coworkers[25,26]) were interpreted as growing nanoparticles of a size defined by $q = 2\pi/d$. These nanoparticles increased monotonically during the initial stages of formation from ~ 5–20 nm and then more rapidly once crystallization was observed in the WAXS.

The validity of these 'Kratky type plot' procedures for the SAXS data does need to be more fully assessed (*e.g.* particle size comparison with SEM or TEM), however the values obtained were at least of the same order as the Scherrer analysis (~ 40 nm) of the initial crystallites. Additionally, Beale *et al.*[67] have obtained reasonable values using the same procedure to examine the formation of ZnAPO-34, whilst Koch *et al.*[66] used a similar procedure to study large macromolecules. These results then indicate that this procedure may offer a reasonable way to obtain at least an estimate of nanoparticle size from dense gels.

The information obtained from the XAS and SAXS, along with an Avrami analysis of the WAXS (indicating diffusion limited processes), the *in situ* spectroscopic Raman (rapid formation of Al–O–P units on mixing of the initial gel phase) and the UV-Vis (complementary observation of initial formation of cobalt hexa-aquo species and the octahedral to tetrahedral conversion), led to the proposed crystallization
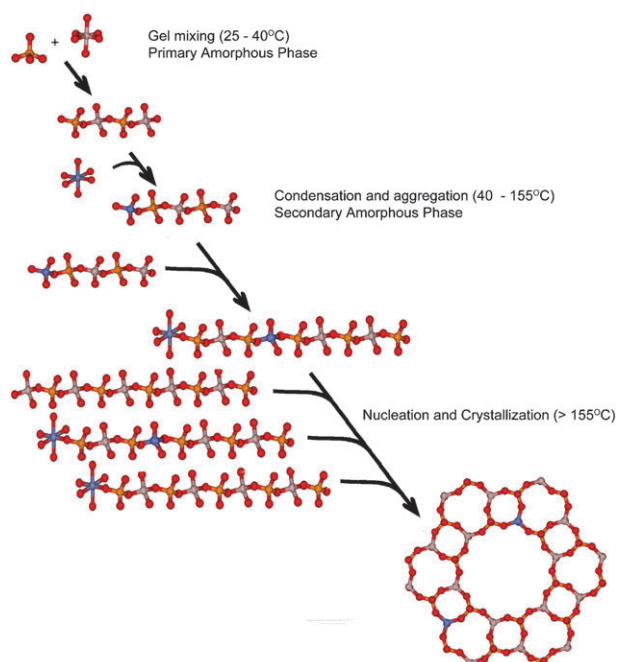
Fig. 10 The hydrothermal synthesis of CoAPO-5 as described by Grandjean *et al.* from their complementary multiple technique studies. Reprinted with modifications with permission from D. Grandjean, A. M. Beale, A. V. Petukhov and B. M. Weckhuysen, *J. Am. Chem. Soc.*, 2005, **127**, 14454–14465. Copyright 2005 American Chemical Society.

model in Fig. 10. Here, reaction of the starting reagents forms a primary amorphous gel which then aggregates into a secondary amorphous phase from 40 to *ca.* 155 °C and then nucleates to form CoAPO-5. The initial incorporation of Co^{2+} into the chains can occur at low temperature *via* the formation of octahedral Co-phosphate species (as indicated in an *in situ* UV-Vis study by Weckhuysen *et al.*[68]). These results are interesting as the authors propose experimental evidence that the formation of chain-like species (*e.g.* Loiseau *et al.*[49] WAX study) are indeed directly involved in a chain formation mechanism of AlPOs as proposed by Oliver *et al.*[50]

Similar measurements were performed by Beale *et al.*[67] on ZnAPO-34, with an even closer match between the SAXS and Scherrer particle size determinations (~ 12 nm), indicating size retention during crystallization and a similar (but this time two stage) crystallization mechanism was proposed. Most importantly, however, this work discussed the role of the Zn^{2+} ions which appear to act as both nucleating *and* structure directing agents—an observation latterly confirmed by the *in situ* Raman measurements of the organic template conformation performed by O'Brien *et al.*[70]

Most recently Simmance *et al.*[71] again utilized combined XAS/WAXS to examine CoAPO-5 formation. Unlike Grandjean *et al.*,[56] no additional techniques were incorporated, however this study represents the first example of *simultaneous* XAS/WAXS measurement. Unlike the previous studies the white line intensity did not show a gradual decrease pre-crystallization but underwent an initial decrease followed by a stabilization and then a more rapid decrease as crystallites where observed. The observation of a stable period

rather than a continuous conversion was interpreted as a conversion of the cobalt centres into a pseudo-octahedral structure partially bonded to phosphorous before converting to the tetrahedral network, rather than a direct octahedral to tetrahedral conversion. The difference between this and the previous studies was attributed to the effect of the different organic template on the cobalt ions in solution and indeed we note that these two systems may provide an interesting target for a study combining *in situ* Raman (to examine the organic-inorganic interaction in more detail) with SAXS/WAXS and EXAFS.

The differences between the studies of Grandjean *et al.*[56] and Simmance *et al.*[71] again demonstrate that, as with the study of clear solutions, whilst the synchrotron (and combined spectroscopic) studies can provide a wealth of information, they cannot always provide the means to fully unravel the formation mechanism. Indeed, a considerable problem with XAS techniques for example is the fact that it is very difficult to probe the *in situ* environment of light elements such as aluminium and silicon which can constitute the majority of the nanoporous framework (*i.e.* zeolite and AlPOs). XANES and EXAFS have therefore generally been restricted to examining 'probe' elements (*e.g.* Zn or Co) substituted in relatively small quantities into the framework.

However, as demonstrated in Fig. 11, Beale *et al.*[72] have devised a setup capable of examining light elements with edge energies as low as 200 eV under *in situ* conditions. Consisting of a 10 mm graphite O ring mounted on top of Teflon, which acts as a spacer between the Teflon and Kapton windows, the cell maintained a hydrothermal environment (*ca.* 2 mm^3) with Kapton thin enough (25 μm) to allow low energy X-ray penetration. It was successfully tested during the crystallization of both CoAPO-5 and AlPO-5 where significant differences in the Al^{3+} local ordering were observed. Distorted tetrahedral or 5-coordinated sites were seen only in the Co system and were attributed to distortions arising from the close attraction of the template to the charged cobalt ions. There was also a significant
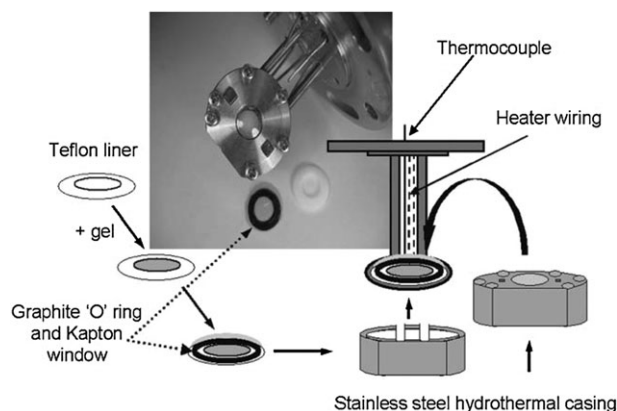

Fig. 11 Schematic of the X-ray absorption cell constructed by Beale *et al.* allowing the study of very light elements that are often part of the CNFM. A. M. Beale, A. M. J. van der Eerden, D. Grandjean, A. V. Petukhov, A. D. Smith and B. M. Weckhuysen, *Chem. Commun.*, 2006, 4410–4412. Reproduced by permission of the Royal Society of Chemistry.

difference in the amount of octahedral Al^{3+} in each system during formation, demonstrating the significant effect of metal substitution on nanoporous materials and indicating that these cannot necessarily be used as a spectroscopic probe as they clearly affect the overall formation process. Techniques that can directly probe any light elements within the nanoporous framework are therefore essential for understanding the local order changes in these materials and understanding the formation process as a whole.

Interestingly, synchrotron-based experiments, which combine XAS, remain relatively underutilized for the study of CNFM formation. This may be partly due to the difficulties in handling dynamic liquid samples (*e.g.* movement and development of pinholes) and also the fact that, even with quick-EXAFS, the XAS is usually performed over several minutes, followed sequentially by the SAXS/WAXS scan, resulting in a relatively low time resolution. The simultaneous XAS/WAXS measurements performed by Simmance *et al.*[71] may therefore provide a more rapid and higher quality solution to this problem in the future.

6. Beyond inorganic frameworks—metal organic hybrids

The majority of the work highlighted above described inorganic zeolite or AlPO frameworks as these are the oldest and most widely studied. Their importance in several industrial processes also ensures that these investigations will continue in an attempt to develop new materials and more efficient synthesis routes. More recently however, inorganic–organic hybrid MOF materials have begun to gain considerable attention[13] as these, along with variants such as zeolitic imidazolate frameworks (ZIFs) and covalent organic frameworks (COFs), may offer advantages in fields such hydrogen storage, CO/CO_2 sequestering and low temperature enzyme like catalysis (*e.g.* Kuppler *et al.*[2] and Blauwhoff *et al.*[3]). To date the majority of this work has focused on the synthesis of new frameworks with interesting properties by simple variation of the synthesis parameters. Some researchers are now however beginning to consider the examination of their fundamental formation process.[73] This area will therefore become one of the next challenges for the *in situ* synchrotron-based setup. Indeed, given the wide range of nanoporous structures MOFs can form under a variety of synthesis conditions it is likely that an even greater array of synthesis mechanisms may operate compared to inorganic frameworks.

Some recent examples of synchrotron based studies in this area have focused on the formation of the MIL series of materials from discrete pre-fabricated SBUs. If these SBUs remain intact, the ability to pre-fabricate them should offer unprecedented rational control over the synthesis process and allow the rational design of CNFMs. To date pseudo *in situ* EXAFS has been used by Surble *et al.*[74] to demonstrate that SBU retention does indeed occur during the formation of MIL-89, however under slightly varied conditions (addition of terephthalic acid) Serre *et al.*[75] have noted the breakdown of the same SBU to form MIL-85. The ambiguity surrounding the role of SBUs and similar precursor units has also been underlined by atomic force microscopy studies of

Shoaee *et al.*[76] where the growth units of the Cu trimesate HKUST-1 were demonstrated to be smaller to those observed in solution.

Currently, Millange *et al.*[61] have performed the only fully *in situ* synchrotron diffraction study of MOF-type materials, examining the formation of MIL-53 with EDXRD. Here a kinetically stabilized intermediate, structurally unrelated to MIL-53 but similar to MOF-235, was observed. This indicates the dissolution, release and rearrangement of the pre-formed SBU components during synthesis. As described in Fig. 12 the work also detailed the formation of the MOF HKUST-1 over several temperatures and used the Avrami model to determine some characteristics of the formation process. An *n* value of 1.5 was observed, which is generally lower than that reported for most inorganic frameworks and is indicative of continuous nucleation. It was also noted that the activation energy appeared to be somewhat higher than similar nucleation controlled growth systems (73.3 kJ mol^{-1}), although, as we have discussed above, it is difficult to draw any further conclusions from such comparisons between systems.

Finally we note that whilst not *in situ* Bajpe *et al.*[77] have for the first time utilized SAXS at room temperature to examine the role of an organic template in the formation of $Cu_3(BTC)_2$ materials containing Keggin-type HPAs
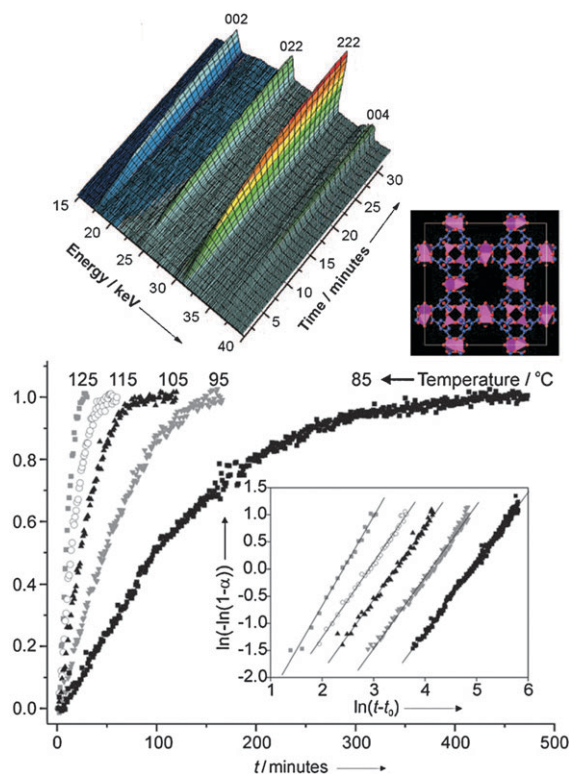

Fig. 12 The first example of a fully *in situ* synchrotron-based study of a MOF material. Here the crystallization of copper carboxylate HKUST-1 was monitored over several temperatures using EDXRD and analyzed using the sharp-Hancock procedure. Figures from F. Millange, M. I. Medina, N. Guillou, G. Férey, K. M. Golden and R. I. Walton, *Angew. Chem., Int. Ed.*, 2010, **49**, 763–766. Copyright Wiley-VCH Verlag GmbH & Co. KGaA. Reproduced with permission.

(where BTC = 1,3,5-benzenetricarboxylic acid and HPA = heteropolyacids). When combined with NMR, DLS and NIR measurements the results show a strong interaction between Cu^{2+} ions and HPA indicating that HPA may act as structure directing agent by defining the position of the Cu^{2+} ions *before* the addition of the BTC organic linker.

As with silicalite, the role of the SBU in these materials may become an area of significant debate, whilst the directing effects of synthesis parameters such as 'templating' agents have only begun to be understood. It is clear therefore that the initial measurements and results discussed in this section are only the 'tip of the iceberg' and that many of the techniques introduced in the tool kit in Table 1 and analysis procedures detailed in the previous sections of this tutorial review will no doubt be applied to these systems in the future.

7. Future perspectives

In situ synchrotron-based techniques are being increasingly employed to examine the formation processes of CNFMs under conditions approaching *in situ*. To date the majority of these have either been single technique setups (*e.g.* WAXS, SAXS or XAS), or have included a combination of several synchrotron techniques (*e.g.* SAXS, WAXS and EXAFS). The combination of many techniques (both synchrotron and spectroscopic-based) into a single measurement environment has however been demonstrated, particularly for AlPOs, and these can provide a method to more easily obtain a detailed and correlated view of the system. To date such setups are generally constructed bespoke for specific measurements. However, the increasing prevalence of synchrotron radiation sources and the requirement for such setups (particularly as these are in demand not only for investigating CNFM formation but also for studying the operation of homogeneous and heterogeneous catalysis) means that these will become more generally available in the future. They will also most likely incorporate more complex experimental cells, allowing the introduction of many of the currently 'independent' techniques described in Table 1 (*e.g.* DLS) into a single measurement system. Of course it must be remembered there will remain a significant number of techniques for which multiple incorporation may prove impossible (*e.g.* it is difficult to envisage a combined SAXS, WAXS, NMR setup) and as such these independent techniques will still be required.

In addition to increasing complexity, the development of faster and more efficient detectors and spectroscopic probes and higher energy, brighter X-ray sources have allowed a continued improvement in the quality and rate of data acquisition of these setups, resulting in more detailed data on the system under investigation. In particular, a move towards very high energy monochromatic synchrotron X-ray sources has recently been observed in the *in situ* heterogeneous catalysis community[16,17] and it is likely that this will also occur in the field of CNFM formation studies. Such setups will not only allow the development of larger more realistic autoclave-like sample environments but also give regular access to some of the less well utilized techniques described in Table 1, such as PDF analysis, which requires high measurement statistics over large scattering vectors.

Aside from improvements in the current setups it is also noted that there has been considerable development in the combination of IR with synchrotron X-rays (*e.g.* Newton *et al.*[78]) and, whilst such setups may not provide a full *in situ* environment or useful information on water-based systems (due to the strong OH signal), they may provide significant information on non-aqueous based systems. In addition STXM, which can provide electronic information on the light elements used for the construction of the some CNTMs (see de Groot *et al.*[79] for a full description of this technique), is included in Table 1 as its development has now reached a stage where particles as small as 12 nm can be imaged and its potential to provide new insight into *in situ* catalytic systems has been demonstrated.[80] Whilst the development of a STXM environment for CNFM synthesis studies remains a considerable challenge, the possibilities for providing new information will be significant.

8. Conclusions

From the examples given in this tutorial review we have demonstrated how synchrotron-based experiments are an essential part of the tool kit required to obtain a more complete understanding of the formation of a nanoporous material. They provide a method for obtaining rapid high quality data under relatively realistic conditions which can be difficult to obtain with non-synchrotron based setups. In addition, when several techniques are combined the data can be easily correlated over several length scales, avoiding inconsistencies in reproducibility which may occur when utilizing several separate measurements. However, this review has also shown that a better understanding of these complex formation processes still requires the inclusion of several independent techniques, either *in situ*, *ex situ* or pseudo *ex situ*. Of course, the development of increasingly complex multiple-techniques setups with higher data quality will increase the amount of understanding that can be obtained from a single experimental measurement, however a comparison of these results with independent measurements will always remains likely.

The examples given here have also demonstrated that their still remains much work to be done to understand the formation of CNFMs and rationalize the reasons for the significant differences between synthesis procedures. This, in combination with the continued development of new self-assembled MOFs means that the future of synchrotron-based studies in this field of research will no doubt remain bright.

Notes and References

1 B. Yilmaz and U. Muller, *Top. Catal.*, 2009, **52**, 888–895.
2 R. J. Kuppler, D. J. Timmons, Q. R. Fang, J. R. Li, T. A. Makal, M. D. Young, D. Yuan, D. Zhao, W. Zhuang and H. Zhou, *Coord. Chem. Rev.*, 2009, **253**, 3042–3066.
3 P. M. M. Blauwhoff, J. W. Gosselink, E. P. Kieffer, S. T. Sie and W. H. J. Stork, in *Catalysis and Zeolites, Fundamentals and Applications*, ed. J. Weitkamp and L. Puppe, Springer, New York, 1999, pp. 437–530.
4 D. W. Lewis, D. J. Willock, C. R. A. Catlow, J. M. Thomas and G. J. Hutchings, *Nature*, 1996, **382**, 604–606.
5 S. M. Auerbach, M. H. Ford and P. A. Monson, *Curr. Opin. Colloid Interface Sci.*, 2005, **10**, 220–225.

6 C. Baerlocher and L. B. McCusker, *Database of Zeolite Structures*: http://www.iza-structure.org/databases/, 2010.

7 W. Vermeiren and J. P. Gilson, *Top. Catal.*, 2009, **52**, 1131–1161.

8 D. Farrusseng, S. Aguado and C. Pinel, *Angew. Chem., Int. Ed.*, 2009, **48**, 7502–7513.

9 M. Eddaoudi, J. Kim, N. Rosi, D. Vodak, J. Wachter, M. O'Keeffe and O. M. Yaghi, *Science*, 2002, **295**, 469–472.

10 C. S. Cundy and P. A. Cox, *Microporous Mesoporous Mater.*, 2005, **82**, 1–78.

11 J. H. Yu and R. R. Xu, *Chem. Soc. Rev.*, 2006, **35**, 593–604.

12 G. Ferey, *Chem. Soc. Rev.*, 2008, **37**, 191–214.

13 B. M. Weckhuysen, *Angew. Chem., Int. Ed.*, 2009, **48**, 4910–4943.

14 The synthesis environment is described in this manner because many syntheses are performed at high temperature and pressure and require thick steel autoclaves which cannot be penetrated by most measurement probes without significant modification.

15 P. Norby, *Curr. Opin. Colloid Interface Sci.*, 2006, **11**, 118–125.

16 K. D. Liss, A. Bartels, A. Schreyer and H. Clemens, *Textures Microstruct.*, 2003, **35**, 219–252.

17 M. G. O'Brien, A. M. Beale, S. D. M. Jacques, M. Di Michiel and B. M. Weckhuysen, *Appl. Catal., A*, 2010, DOI: 10.1016/j.apcata.2010.06.027.

18 B. J. Schoeman, J. Sterte and J. E. Otterstedt, *Zeolites*, 1994, **14**, 110–116.

19 C. S. Cundy and P. A. Cox, *Chem. Rev.*, 2003, **103**, 663–701.

20 P. A. Wright, *Microporous Framework Solids*, RSC Publishing, Cambridge, 2008.

21 This three letter code represents the framework topology of the zeolite. This is the unique organization of repeating atoms that form a series of 1, 2 or 3 dimensional channels and cages. For a full list of these codes please see: http://www.iza-structure.org/databases/.

22 O. Glatter and O. Kratky, *Small Angle X-ray Scattering*, Academic Press, London, 1982, available at: http://physchem.kfunigraz.ac.at/sm/Software.htm.

23 D. I. Svergun and M. H. J. Koch, *Curr. Opin. Struct. Biol.*, 2002, **12**, 654–660.

24 W. Clegg, A. J. Blake, R. O. Gould and P. Main, *Crystal Structure Analysis Principles and Practice*, Oxford University Press, Oxford, 2001.

25 P. de Moor, T. P. M. Beelen, R. A. van Santen, L. W. Beck and M. E. Davis, *J. Phys. Chem. B*, 2000, **104**, 7600–7611.

26 P. de Moor, T. P. M. Beelen, B. U. Komanschek, L. W. Beck, P. Wagner, M. E. Davis and R. A. van Santen, *Chem.–Eur. J.*, 1999, **5**, 2083–2088.

27 O. Regev, Y. Cohen, E. Kehat and Y. Talmon, *Zeolites*, 1994, **14**, 314–319.

28 B. J. Schoeman, *Zeolites*, 1997, **18**, 97–105.

29 W. H. Dokter, H. F. Vangarderen, T. P. M. Beelen, R. A. Van Santen and W. Bras, *Angew. Chem., Int. Ed. Engl.*, 1995, **34**, 73–75.

30 G. Sankar and W. Bras, *Catal. Today*, 2009, **145**, 195–203.

31 S. L. Burkett and M. E. Davis, *Chem. Mater.*, 1995, **7**, 1453–1463.

32 V. Nikolakis, D. G. Vlacho and M. Tsapatsis, *Microporous Mesoporous Mater.*, 1998, **21**, 337–346.

33 C. H. Cheng, G. Juttu, S. F. Mitchell and D. F. Shantz, *J. Phys. Chem. B*, 2006, **110**, 21430–21437.

34 W. Fan, M. O'Brien, M. Ogura, M. Sanchez-Sanchez, C. Martin, F. Meneau, K. Kurumada, G. Sankar and T. Okubo, *Phys. Chem. Chem. Phys.*, 2006, **8**, 1335–1339.

35 A. Aerts, L. R. A. Follens, M. Haouas, T. P. Caremans, M. A. Delsuc, B. Loppinet, J. Vermant, B. Goderis, F. Taulelle, J. A. Martens and C. E. A. Kirschhock, *Chem. Mater.*, 2007, **19**, 3448–3454.

36 A. Aerts, M. Haouas, T. P. Caremans, L. R. A. Follens, T. S. van Erp, F. Taulelle, J. Vermant, J. A. Martens and C. E. A. Kirschhock, *Chem.–Eur. J.*, 2010, **16**, 2764–2774.

37 T. M. Davis, T. O. Drews, H. Ramanan, C. He, J. S. Dong, H. Schnablegger, M. A. Katsoulakis, E. Kokkoli, A. V. McCormick, R. L. Penn and M. Tsapatsis, *Nat. Mater.*, 2006, **5**, 400–408.

38 S. Kumar, Z. P. Wang, R. L. Penn and M. Tsapatsis, *J. Am. Chem. Soc.*, 2008, **130**, 17284–17286.

39 J. M. Fedeyko, D. G. Vlachos and R. F. Lobo, *Langmuir*, 2005, **21**, 5197–5206.

40 C. E. A. Kirschhock, S. P. B. Kremer, J. Vermant, G. Van Tendeloo, P. A. Jacobs and J. A. Martens, *Chem.–Eur. J.*, 2005, **11**, 4306–4313.

41 S. L. Burkett and M. E. Davis, *J. Phys. Chem.*, 1994, **98**, 4647–4653.

42 L. Gora, K. Streletzky, R. W. Thompson and G. D. J. Phillies, *Zeolites*, 1997, **18**, 119–131.

43 S. Mintova, N. H. Olson, V. Valtchev and T. Bein, *Science*, 1999, **283**, 958–960.

44 R. Grizzetti, G. Artioli, M. Gemmi, F. Carsughi and P. Riello, in *Recent Advances in the Science and Technology of Zeolites and Related Materials, Pts a-c*, Elsevier Science, Amsterdam, 2004, vol. 154, pp. 355–363.

45 M. G. O'Brien, A. M. Beale, B. W. M. Kuipers, B. H. Erne, D. W. Lewis and C. R. A. Catlow, *J. Phys. Chem. C*, 2009, **113**, 18614–18622.

46 W. Fan, M. Ogura, G. Sankar and T. Okubo, *Chem. Mater.*, 2007, **19**, 1906–1917.

47 H. Y. He, P. Barnes, J. Munn, X. Turrillas and J. Klinowski, *Chem. Phys. Lett.*, 1992, **196**, 267–273.

48 R. I. Walton, F. Millange, D. O'Hare, A. T. Davies, G. Sankar and C. R. A. Catlow, *J. Phys. Chem. B*, 2001, **105**, 83–90.

49 T. Loiseau, L. Beitone, F. Millange, F. Taulelle, D. O'Hare and G. Ferey, *J. Phys. Chem. B*, 2004, **108**, 20020–20029.

50 S. Oliver, A. Kuperman and G. A. Ozin, *Angew. Chem., Int. Ed.*, 1998, **37**, 47–62.

51 A. Guinier, *X-ray Diffraction in Crystals, Imperfect Crystals and Amorphous Bodies (Reprint)*, Dover Publications, New york, 1995.

52 A. L. Patterson, *Phys. Rev.*, 1939, **56**, 978.

53 J. L. Schlenker and B. K. Peterson, *J. Appl. Crystallogr.*, 1996, **29**, 178–185.

54 D. Chiche, M. Digne, R. Revel, C. Chanéac and J. Jolivet, *J. Phys. Chem. C*, 2008, **112**, 8524–8533.

55 A. N. Christensen, T. R. Jensen, P. Norby and J. C. Hanson, *Chem. Mater.*, 1998, **10**, 1688–1693.

56 D. Grandjean, A. M. Beale, A. V. Petukhov and B. M. Weckhuysen, *J. Am. Chem. Soc.*, 2005, **127**, 14454–14465.

57 R. J. Francis, S. O'Brien, A. M. Fogg, P. S. Halasyamani, D. O'Hare, T. Loiseau and G. Ferey, *J. Am. Chem. Soc.*, 1999, **121**, 1002–1015.

58 J. H. Hancock and J. D. Sharp, *J. Am. Ceram. Soc.*, 1972, **55**, 74.

59 S. F. Hulbert, *Journal of the British Ceramic Society*, 1969, **6**, 11.

60 M. G. O'Brien, M. Sanchez-Sanchez, A. M. Beale, D. W. Lewis, G. Sankar and C. R. A. Catlow, *J. Phys. Chem. C*, 2007, **111**, 16951–16961.

61 F. Millange, M. I. Medina, N. Guillou, G. Férey, K. M. Golden and R. I. Walton, *Angew. Chem., Int. Ed.*, 2010, **49**, 763–766.

62 A. Gualtieri, P. Norby, G. Artioli and J. Hanson, *Phys. Chem. Miner.*, 1997, **24**, 191–199.

63 R. W. Thompson and A. Dyer, *Zeolites*, 1985, **5**, 202–210.

64 R. W. Thompson and A. Dyer, *Zeolites*, 1985, **5**, 292–301.

65 J. M. Thomas and G. Sankar, *J. Synchrotron Radiat.*, 2001, **8**, 55–60.

66 G. Sankar, J. M. Thomas, F. Rey and G. N. Greaves, *J. Chem. Soc., Chem. Commun.*, 1995, 2549–2550.

67 A. M. Beale, A. M. J. van der Eerden, S. D. M. Jacques, O. Leynaud, M. G. O'Brien, F. Meneau, S. Nikitenko, W. Bras and B. M. Weckhuysen, *J. Am. Chem. Soc.*, 2006, **128**, 12386–12387.

68 M. H. J. Koch, P. Vachette and D. I. Svergun, *Q. Rev. Biophys.*, 2003, **36**, 147–227.

69 B. M. Weckhuysen, D. Baetens and R. A. Schoonheydt, *Angew. Chem., Int. Ed.*, 2000, **39**, 3419–3422.

70 M. G. O'Brien, A. M. Beale, C. R. A. Catlow and B. M. Weckhuysen, *J. Am. Chem. Soc.*, 2006, **128**, 11744–11745.

71 K. Simmance, G. Sankar, R. G. Bell, C. Prestipino and W. van Beek, *Phys. Chem. Chem. Phys.*, 2010, **12**, 559–562.

72 A. M. Beale, A. M. J. van der Eerden, D. Grandjean, A. V. Petukhov, A. D. Smith and B. M. Weckhuysen, *Chem. Commun.*, 2006, 4410–4412.

73 R. E. Morris, *ChemPhysChem*, 2009, **10**, 327–329.

74 S. Surble, F. Millange, C. Serre, G. Ferey and R. I. Walton, *Chem. Commun.*, 2006, 1518–1520.

75 C. Serre, F. Millange, S. Surble and G. Ferey, *Angew. Chem., Int. Ed.*, 2004, **43**, 6286–6289.

76 M. Shoaee, M. W. Anderson and M. P. Attfield, *Angew. Chem., Int. Ed.*, 2008, **47**, 8525–8528.

77 S. R. Bajpe, C. E. A. Kirschhock, A. Aerts, E. Breynaert, G. Absillis, T. N. Parac-Vogt, L. Giebeler and J. A. Martens, *Chem.–Eur. J.*, 2010, **16**, 3926–3932.

78 M. A. Newton, M. Di Michiel, A. Kubacka and M. Fernandez-Garcia, *J. Am. Chem. Soc.*, 2010, **132**, 4540–4541.

79 F. M. F. de Groot, E. de Smit, M. M. van Schooneveld, L. R. Aramburo and B. M. Weckhuysen, *ChemPhysChem*, 2010, **11**, 951–962.

80 E. de Smit, I. Swart, J. F. Creemer, G. H. Hoveling, M. K. Gilles, T. Tyliszczak, P. J. Kooyman, H. W. Zandbergen, C. Morin, B. M. Weckhuysen and F. M. F. de Groot, *Nature*, 2008, **456**, 222–225.